Equation (8) combined with (7) gives α and β. I_{corr} can be evaluated from α and β using (6).

Method (iii)

$\tilde{I}_2$ and $\tilde{I}_3$ are measured at $\eta = 0$, then

$$\frac{6(\tilde{I}_3)_{\eta=0}}{\varepsilon_p(\tilde{I}_2)_{\eta=0}} = -\frac{(\alpha-\beta)^2+\alpha\beta}{(\alpha-\beta)}. \quad (9)$$

Using (7) and (9) one can get α and β hence I_{corr}.

The system chosen for evaluating the method is mild steel in IN sulphuric acid. The cell design is according to ASTM G-72. The sample used as a working electrode is a rectangular strip which is masked off with araldite everywhere except at the bottom to expose a fixed area. Platinum strips are used as a counter electrode and SCE as a reference electrode.

A sinusoidal signal of 10 mV RMS and a frequency of 42 Hz is derived from a low distortion (0·05 %) Aplab (Type AG 3) oscillator. This is applied to the system through a high stability potentiostat designed for this purpose. The cell response is passed through tuned amplifiers to separate second and third harmonic components.

Figure 1 shows the plot of $\tilde{I}_2$ against η_a and η_c. Since $\tilde{I}_2$ decreases with increasing η_c and the reverse is the case with η_a, it is concluded that $\alpha < \beta$.

The results obtained by various methods are shown

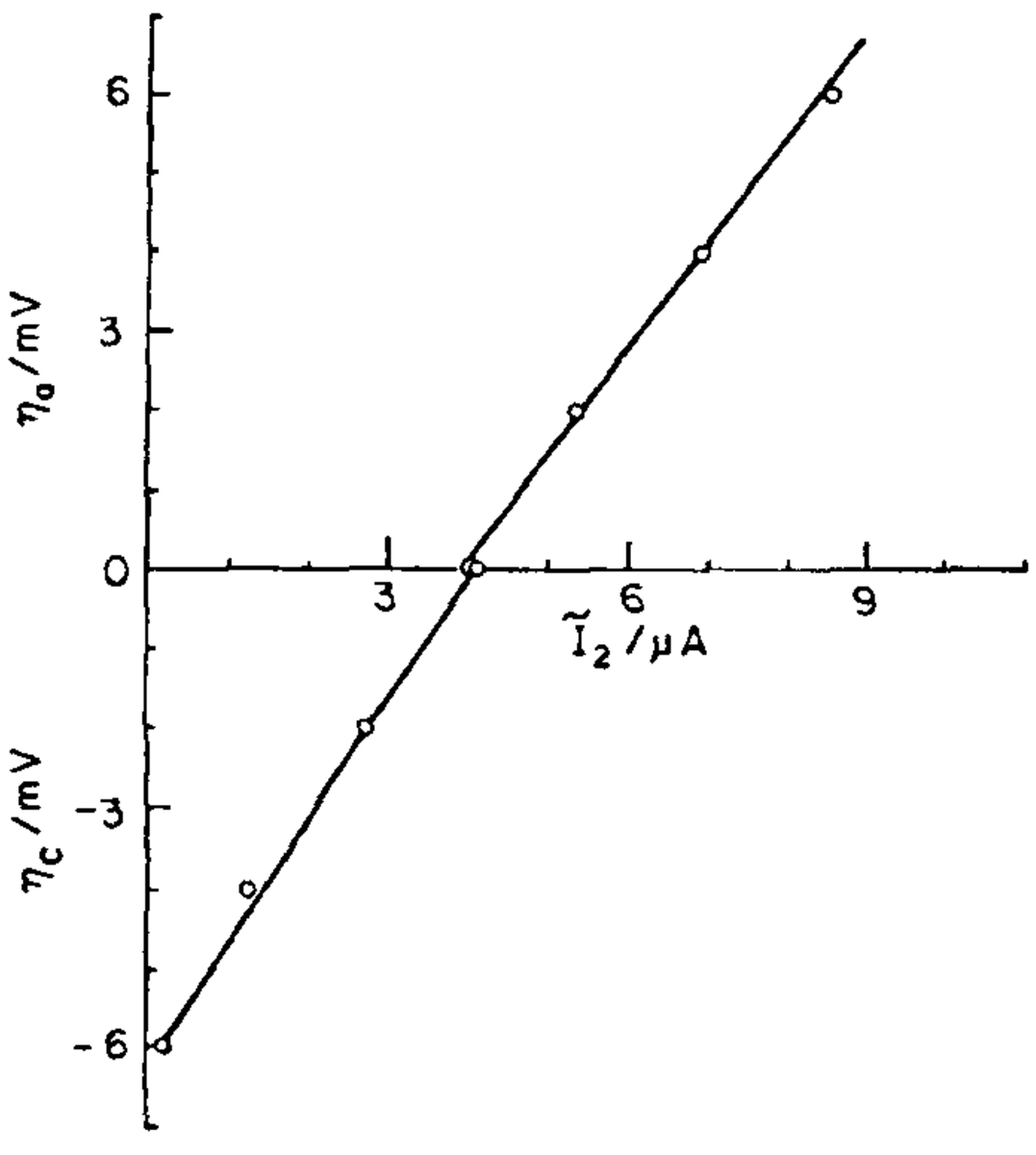

Figure 1. I_2 *vs* η_a (upper) and I_2 *vs* η_c (lower) curves for mildsteel in IN sulphuric acid. E_p = 14 mV, Electrode area = 1.2 cm^2.

Table 1 *Comparison of Corrosion rate for Mild steel in 1 N sulphuric acid obtained by different methods.*

Method	I_{corr} μA/cm^2
$\tilde{I}_2$ vs η_c and polarisation resistance	361
$\tilde{I}_2$ vs η_a and polarisation resistance	398
$(\eta)\tilde{I}_2 = 0$ and polarisation resistance	390
$\tilde{I}_2$ and $\tilde{I}_3$ and polarisation resistance	389
Logarithmic polarisation	358
Linear polarisation (using α and β from logarithmic polarisation)	340

in table 1. These values are in good agreement with the corrosion rate obtained by classical polarisation methods.

Following are the advantages of the proposed method:

(i) Since d.c. polarisation involved is around 10 mV, surface morphology is not affected.

(ii) α and β are obtained close to corrosion potential which is an advantage over logarithmic polarisation method.

(iii) The method is quite fast and measurements can be done in approximately 10 minutes.

The authors thank Prof. S. Satyanarayana for his help in formulating the theory of the method and for valuable discussions. Thanks are due to Dr Prabhakar Rao for providing the reprint of the paper cited in Ref. 1.

22 September 1983

1. Prabhakar Rao, G. and Mishra, A. K., *J. Electroanal-Chem.*, 1977, **77**, 121.
2. Devay, J. and MesZaros, I., *Acta Chim. Acad. Sci. Hung.*, 1979, **84**, 100.

LATTICE THERMAL CONDUCTIVITY OF GERMANIUM AT LOW TEMPERATURES

R. P. GAROLA
Department of Physics, Garhwal University, Srinagar, Garhwal 246 174, India.

LATTICE thermal conductivity of germanium and other non-metallic solids has been widely studied by many workers[1-3] in the past, using Callaway's model[4] and modifications thereof. In all these studies, it has been implicitly assumed that the relaxation rates due to

isotopic impurities ($\tau_D^{-1} \sim Aw^4$) and anharmonic interactions ($\tau_A^{-1} \sim Bw^2T^3$) are independent of each other, which are then added in accordance with Mathiessen's rule[5] and no interference or cross term[6] of defect and anharmonic interactions appear in the total relaxation time. However, these cross-terms (Γ^{AD}) cannot be ignored in the exact calculation of thermal conductivity of doped crystals, particularly near the low temperature maximum, where the conventional domination of τ_D^{-1} ends and that of τ_A^{-1} starts. The results of a more careful study, which includes these cross terms in the calculations of thermal conductivity of germanium at low temperatures, are reported here.

It has been remarked earlier[6] that the cross term Γ^{AD} is ignored by earlier workers in conductivity formulations because it does not appear owing to the neglect of anharmonicity, whenever isotopic impurities are accounted in the Hamiltonian[7]. But if the anharmonic terms are retained along with the defect terms in the crystal Hamiltonian, we obtain[6] the cross term Γ^{AD}, appearing in the expression for phonon width, which is given as,

$$\Gamma^{AD}(w) = (3\lambda V k_B T/\pi^5 \hbar w_L^2)\theta(w_L - w_k) \int \sin\theta \, d\theta \, d\phi \int |C(-k, k_1)|^2 w_{k_1}^2 \, dw_{k_1}, \quad (1)$$

where λ is a dimensionless parameter, V the crystal volume, $w_L = (4\gamma/M)^{1/2}$; γ being the harmonic force constant, θ is the Heaviside step function and $C(k_1, k_2)$ is mass change parameter discussed elsewhere[6]. After carrying out the integration in (1) and taking the directional average over all possible atomic configurations, it is seen that $\Gamma^{AD}(w) \sim Dw^3T$, where D is the interaction parameter, which for a linear chain model[8], is given by $D = (3k_B/32\pi^3\hbar)\lambda$. A; with $A = (V/12N\pi v^3)(M_0/\mu)^2 f(1-f)$, the symbols having their usual meaning[6]. The interaction parameter D, as given above, depends on λ, the dimensionless cubic anharmonic parameter and A, the defect parameter depending upon the impurity concentration.

Let us now calculate thermal conductivity of Ge, using Callaway's expression[4],

$$K(T) = (k_B/2\pi^2 v) \int_0^{w_D} \tau(w)(\hbar w_k/k_B T)^2 \exp(\beta\hbar w k)[\exp(\beta\hbar w_k^{-1}]^{-2} w_k^2 \, dw_k, \quad (2)$$

where the effective relaxation time $\tau(w)$ now also includes the cross term Γ^{AD} and is given by,

$$\tau^{-1}(w) = (v/FL) + Aw^4 + Bw^2T^3 + Dw^3T. \quad (3)$$

The different parameters used in the present analysis are listed in table 1; figure 1 shows the theoretically analyzed curves for Ge along with the experimental points of Holland[9]. If the interaction term Dw^3T is neglected (*i.e.* using Callaway's model) the conductivity curve reaches a higher value in the vicinity of low temperature maximum $K_m(T)$ as shown by dotted curve in figure 1. Using Callaway's model, to analyze thermal conductivity data, one often observes a deviation near $K_m(T)$ as also pointed out elsewhere[9,10]. One has then to readjust the values of parameters F, A and B in order to get a best fit. However, if the cross term Dw^3T is considered, a good agreement between theory and experiment is found, as indicated by the continuous curve in figure 1. We have used $D = 1.203 \times 10^{-33}$ sec^2 k^{-1}, to get a best fit.

Table 1 *Values of different parameters*

v	3.5×10^5 cm/sec
L	0.24 cm
F	0.8
θ_D	376°K
A	2.4×10^{-44} sec^3
B	2.77×10^{-23} sec K^{-3}
D	1.203×10^{-33} sec^2 K^{-1}

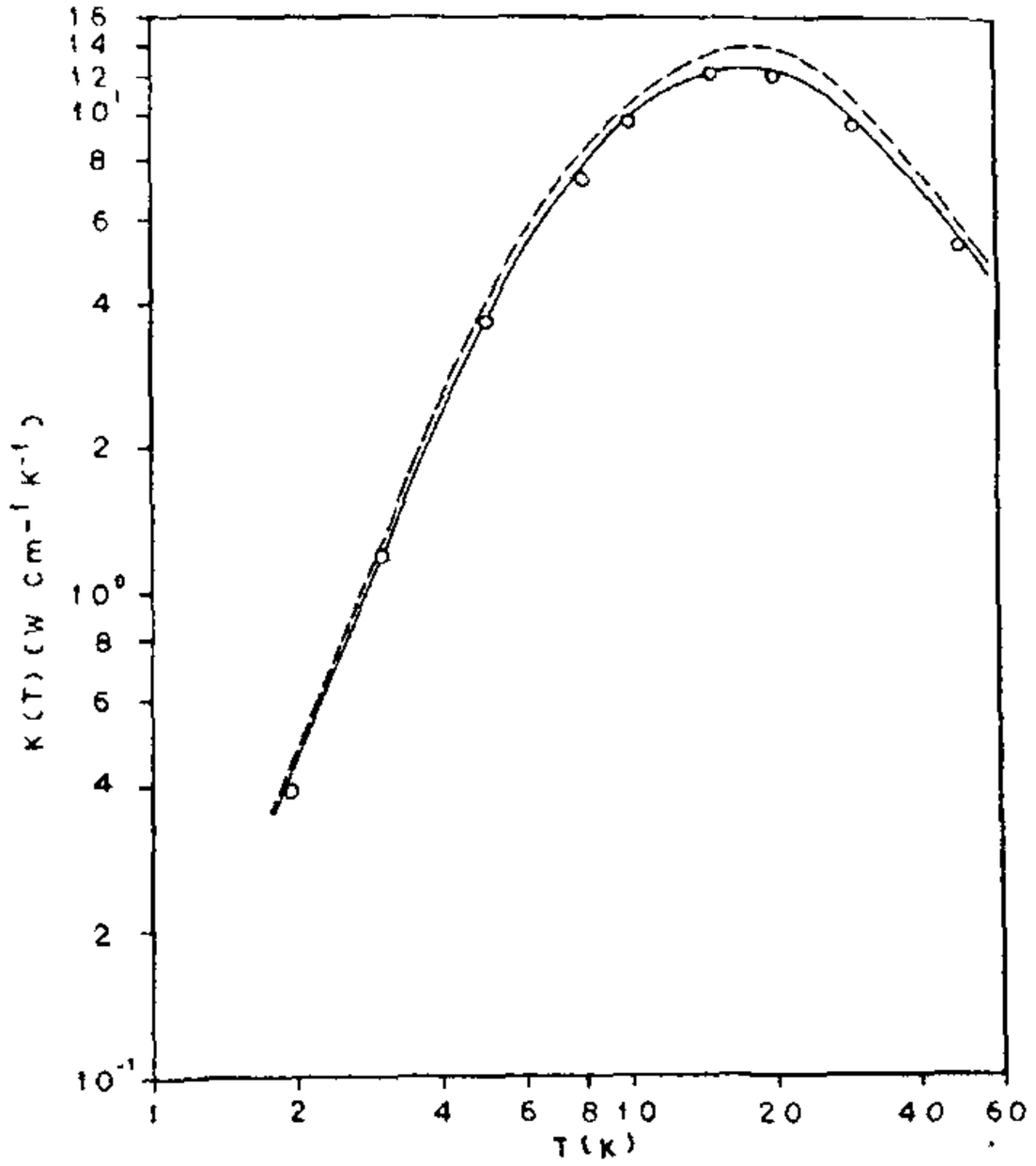

Figure 1. Thermal conductivity curves for germanium, open circles are the experimental points from Ref. 9. Dotted curve shows the conductivity without Dw^3T term and continuous curve is the present analysis.

Recently, it has been shown by Srivastav and Kumar[10] that the deviation near $K_m(T)$ could be accounted by including an interference term ξ in the analysis which is taken as a constant (0.15 for Ge) but it appears to be contradictory since ξ depends on T considerably, as evident from their equation (20). From the present work it is concluded that the deviation near $K_m(T)$ could be attributed to the neglect of the cross term, between defect and anharmonic parameters, which varies as Dw^3T. The present analysis is also valid for other non-metallic solids doped with isotopic impurities.

30 December 1983

1. Carruthers, P., *Rev. Mod. Phys.*, 1961, **33**, 92.
2. Klemens, P. G., *Solid State Phys.*, (eds) F. Seitz and D. Turnbull, Academic Press, New York, 1958, **7**, p. 1.
3. Martin, J. J., *J. Phys. Chem. Solids*, 1972, **33**, 1139.
4. Callaway, J., *Phys. Rev.*, 1959, **B113**, 1046.
5. *Ziman, J. M., Electrons and phonons*, Oxford University Press, N. Y.
6. Garola, R. P., *Acta. Phys. Polonica*, 1983, **A63**, 121.
7. Maradudin, A. A., *J. Am. Chem. Soc.*, 1964, **86**, 3405.
8. Pathak, K. N., *Phys. Rev.*, 1965, **A139**, 156.
9. Holland, M. G., *Phys. Rev.*, 1963, **132**, 2461.
10. Srivastav, G. C. and Kumar, Anil, *Phys. Rev.*, 1982, **B25**, 2560.

A NEW FLAVONE GLYCOSIDE FROM *MELIA AZEDARACH* LINN.

MAMTA MISHRA and
SANTOSH K. SRIVASTAVA
Department of Chemistry, University of Saugar, Sagar 470 003, India.

FROM the stem bark of *Melia azedarach*, we report the isolation and characterization of a new flavone glycoside; 4′-5-dihydroxy flavone-7-O-α-L-rhamnopyranosyl- (1 → 4)-β-D-glucopyranoside (I) on the basis of spectral and chemical evidence.

The air-dried and powdered stem-bark of *M. azedarach*[1,2] (5 kg) was extracted five times with rectified spirit under reflux for 20 days. The total spirit extract (40 lit.) was concentrated under reduced pressure to a small volume (400 ml) and poured into water (1 lit.). The water insoluble fraction was extracted with different organic solvents in the order of their increasing polarities. Ethyl acetate extract gave a compound which after purification by column chromatography (SiO_2-gel; EtOAc: Me_2CO; 8:2) yielded a reddish-yellow crystalline product (Me_2CO:MeOH), (yield 1.6 g), mp, 208–10° which was found to be a single entity on PC [R_f, 0.92, (*n*-BAW 4:1:5) and 0.78 (15% gl AcOH)] and TLC [R_f, 0.85, (MeOH:$CHCl_3$, 5:3) and 0.77 (MeOH:$CHCl_3$, 4:7)], IR ν_{max}^{KBr} 825, 665, 1050, 1125, 1375, 1380, 1460, 1510, 1610, 1665, 3360–3400 (br) cm^{-1}; UV λ_{max}, 265, 315 (MeOH); 260 (sh), 280, 300, 335, 380 (MeOH + $AlCl_3$); 277, 295 (sh), 360 (MeOH + NaOAc); 270, 332 (NaOMe); [Found: C, 56.20; H, 5.19; $C_{27}H_{30}O_{14}$ reqd; C, 56.05; H, 5.20%]. It gave Shinoda's[3] and Molisch's tests for a flavone glycoside. Acid-hydrolysis (50 ml; 7% H_2SO_4) of the glycoside (900 mg) gave an aglycone, mp, 347–48°, D-glucose (R_f; 0.18, *n*-BAW, 4:1:5 and CO-PC)[4] and L-rhamnose (R_f; 0.38; *n*-BAW, 4:1:5 and CO-PC).[4]

The aglycone was recovered as usual and crystallized from EtOAc:petroleum ether as yellow needles; $C_{15}H_{10}O_5$ (M^+ at m/e 270); IR ν_{max}^{KBr}, 1050, 1220, 1385, 1460, 1500, 1600, 1660, 1605 and 3440 (br) cm^{-1}; UV λ_{max}, 265, 325 (MeOH); 264, 375 (MeOH + NaOMe) 276, 345 (MeOH + $AlCl_3$); 260, 335 (H_3BO_3 – NaOMe); 286, 336 (MeOH + NaOAc) nm; MS at m/e; 270 (100%), 269 (13%), 242 (19%), 152 (16%), 149 (10%), 146 (18%), 118 (16%) and 117 (22%);[5] and ^{1}H NMR (δ, $CDCl_3$), 6.22 (d, J = 2 H_z, H-6), 6.48 (d, J = 2 H_z, H-8), 6.70 (s, H-3), 7.90 (d, J = 9 H_z, H-2′ and H-6′), 6.95 (d, J = 9 H_z, H-3′ and 5′), 12.90 (s, OH); [Found: C, 66.60; H, 3.68; $C_{15}H_{10}O_5$; reqd; C, 66.66; H, 3.70%]; triacetate (100 mg of the aglycone + 5 ml of Ac_2O + 5 ml C_6H_5N; yield 60 mg); [Found; C, 63.60; H, 4.00; OAc, 32.60; $C_{21}H_{16}O_8$ reqd., C, 63.63; H, 4.04; 3XOAc, 32.57%]; trimethyl ether (100 mg of the aglycone + 5 ml of Me_2SO_4 + 2 g K_2CO_3; yield, 65 mg), mp, 155–56°; [Found: C, 69.20; H, 5.10; OMe, 29.78; $C_{18}H_{16}O_5$ reqd; C, 69.23; H, 5.12; 3XOMe, 29.80%]. The aglycone gave a bathochromic shift with $AlCl_3$ (λ_{max} 276, 345 nm) and NaOAc (λ_{max} 286, 336 nm) which were clear indication for the presence of two hydroxyls at C-5 and C-7 respectively. KOH degradation (50%)[6] of the aglycone yielded phloroglucinol, mp, 216–17° (lit. mp, 217°, mmp and CO-TLC) and *p*-hydroxybenzoic acid, mp, 212–13° (lit. mp, 214°, mmp and CO-TLC), while $KMnO_4$ oxidation afforded *p*-hydroxybenzoic acid (mmp and CO-TLC) as their identifiable oxidation products. Thus, the structure of the aglycone was assigned as apigenin, which